Published as: *Eur J Neurosci*. 2010 June ; 31(12): 2279–2291.

Multi-array silicon probes with integrated optical fibers: light-assisted perturbation and recording of local neural circuits in the behaving animal

Sébastien Royer[1,2], **Boris V. Zemelman**[1], **Mladen Barbic**[1], **Attila Losonczy**[3], **György Buzsáki**[1,2], and **Jeffrey C. Magee**[1]

[1]Howard Hughes Medical Institute, Janelia Farm Research Campus, Ashburn, VA 20147

[2]Center for Molecular and Behavioral Neuroscience, Rutgers, The State University of New Jersey, 197 University Avenue, Newark, NJ 07102 New Jersey

[3]Columbia neuroscience department, Columbia University, NY

Abstract

Recordings of large neuronal ensembles and neural stimulation of high spatial and temporal precision are important requisites for studying the real-time dynamics of neural networks. Multiple shank silicon probes enable large-scale monitoring of individual neurons. Optical stimulation of genetically targeted neurons expressing light sensitive channels or other fast (milliseconds) actuators offers the means for controlled perturbation of local circuits. Here we describe a method to equip the shanks of silicon probes with micron-scale light guides for allowing the simultaneous use of both approaches. We then show illustrative examples of how these compact hybrid electrodes can be used in probing local circuits in behaving rats and mice. A key advantage of these devices is the enhanced spatial precision of stimulation that is achieved by delivering light close to the recording sites of the probe. When paired with the expression of light sensitive actuators within genetically specified neuronal populations, these devices allow the relatively straightforward and interpretable manipulation of network activity.

Keywords

circuit analysis; optrode; ChR2; halorhodopsin; excitation; inhibition

One of the important challenges in neuroscience is to identify the causal links between the collective activity of neurons and behavior. While the study of correlations between ensemble neuronal activity and behavior has produced unprecedented progress in the past decade (Buzsaki et al., 1992; Wilson and McNaughton, 1993; Yamamoto and Wilson, 2008; Battaglia et al., 2009, Harris et al., 2003; Rizk et al., 2009; Gelbard-Sagiv et al., 2008), the correlational nature of these measurements leaves ambiguous the cause and effect relationship. A more thorough understanding requires at least two additional steps. The first one is the identification of the multiple neuronal cell types that uniquely contribute to the assembly behavior – literally like members of an orchestra. There are at least two dozen excitatory and inhibitory neuron types in the cortex with diverse targets, inputs and uniquely tuned biophysical properties and existing methods have serious limitations for identifying

Corresponding authors: Jeffrey Magee, Howard Hughes Medical Institute, Janelia Farm Research Campus, Ashburn, VA 20147, Tel: (571) 209-4123, Fax: (571) 209-4064, mageej@janelia.hhmi.org, Or György Buzsáki, Center for Molecular and Behavioral Neuroscience, Rutgers University, 197 University Avenue, Newark, NJ 07102, Tel: (973) 353-3638, Fax: (973) 353-1820, buzsaki@axon.rutgers.edu.

and segregating these neuron types (Freund et al., 1996; Markram et al., 2004; Klausberger et al., 2003; Klausberger and Somogyi, 2008). The second step is a principled manipulation of the spiking activity of these identified cell groups.

The recently developed molecular optogenetic tools provide a means to achieve each of the above experimental goals (O'Connor et al., 2009; Deisseroth et al., 2006; Zhang et al., 2007a). Optical stimulation of genetically targeted neurons expressing light sensitive channelrhodopsin (ChR2) has recently been reported as a rapid activator of neuronal firing with potential cell type selectivity (Boyden et al., 2005; Han and Boyden, 2007; Ishizuka et al., 2006; Li et al., 2005; Nagel et al., 2003; Zhang et al., 2007b). Rapid silencing of neurons by light-activated chloride pumps such as halorhodopsins (Halo/NpHR) is another powerful approach for perturbing local networks (Han and Boyden, 2007; Zhang et al., 2007b). Several recent papers have demonstrated the feasibility of combining the light activation/silencing of neuronal populations with the recording of neuronal activity in both in vitro and in vivo preparations (Han et al., 2009; Sohal et al., 2009; Jessica et al., 2009). For the in vivo studies, however, the distance between the stimulation and recording sites was relatively large, necessitating the use of large amplitude light intensities (>30 mW) to stimulate the neurons within the recorded area. Among other problems, such imprecise stimulation hinders the clean separation of local and more global network effects. In this article we describe the fabrication and example applications of integrated miniature optoelectronic devices that enable both large neuronal ensemble recordings and simultaneous localized optical perturbation of neurons in behaving animals (A brief description of these methods have been reported; Royer et al., 2008).

Methods and Results

All experiments were conducted in accordance with institutional regulations (Janelia Farm Institutional Animal Care and Use Committee).

Construction of the fiber-based optoelectronic probes

To obtain devices (fiber-based optoelectronic probes or ‘optrode’, Deisseroth et al., 2006; Zhang et al., 2007a) that enable both the recording and optical stimulation of local populations of neurons, we equipped commercially available silicon probes with micron-scale light guides by placing chemically etched optical fibers onto their shanks. The silicon probe models we used (Buzsaki32; Buzsaki64 from NeuroNexus Inc., Ann Arbor, MI) have either 4 or 8 shanks. The shanks are 250 μm apart from each other and bear 8 recording sites each (160 μm^2 each site; 1-3 MΩ impedance) arranged in a staggered configuration (20 μm vertical separation; Fig. 1C, Bartho et al., 2004). An 8-shank silicon probe records from 50 to 140 well-clustered neurons in the hippocampus and neocortex (Fujisawa et al., 2007; Pastalkova et al., 2008). As light guides, we used single mode optical fibers (125 μm in diameter; Thorlabs #460HP), because their light guiding properties are less affected by the etching due to their small core diameter (3.5 μm).

Because light is emitted from the fiber end with the shape of a cone (~30 degree angle), the volume of excited tissue at the level of the recording sites depends on how far above them the fiber ends. For some applications, light modulation needs to be restricted only to the brain volume monitored by the silicon probe, which means that the optical fiber should end <100 μm above the recording sites. However, a critical factor to record numerous neurons is the small size and smooth profile of the electrode, which minimize capillary and neuronal damage during penetration in the brain (Buzsaki, 2004; Kipke et al., 2008). To meet this requirement, the single-mode optical fiber is etched by dipping it into the concentrated hydrofluoric acid. An 8-cm fiber is attached to a micromanipulator and approximately 5 mm of the end is inserted into the acid for 15 to 30 min periods, until the desired 5-20 μm

diameter is achieved (Fig. 1A). After rinsing in distilled water, the tip of the tapered end is cut by a diamond knife to provide a sharp clean edge while the non-etched end of the fiber is glued into a connector (LC type, Thorlabs #86024-5500) and polished following standard procedures (as described in 'Fiber polishing notes', Thorlabs #FN96A).

The next step is to place the optical fiber on the shank of the silicon probe. This procedure is carried out with the help of micromanipulators and under microscopic vision. The silicon probe is placed horizontally and the fiber is positioned with a slight angle (15-20°) with the etched tip touching the shank at the desired distance from the recording sites. Then the remaining part of the fiber is pushed down with a piece of metal micro-tube so that it lies parallel to the surface of the shank (Fig. 1B). Once the fiber is in place, ultraviolet (UV) light-curable glue (Thorlabs #NOA61) is applied by hand to the fiber and shank using a single bristle of a cotton swab. After successful application, UV light (Thorlabs #CS410) is applied for 5 min. This procedure can be done in multiple steps by repeating the process of pushing and gluing the fiber gradually upwards along the shank. Finally, the non-etched portion of the fiber is glued to the bonding area of the probe to provide secure connection. To avoid breakage of the fiber during handling and implantation, the connector end of the fiber and the probe base are interconnected with a metallic bar or/and dental cement (Fig. 2A).

We made different designs of integrated fiber-based optoelectronic silicon devices to address different sets of questions (Fig. 2). Either one or four shanks were equipped with optical fibers, and the distance between the fiber tip and the recording sites varied from 100 to 300 μm, depending on the desired volume of stimulated tissue. For experiments requiring the stimulation of neurons located below the recording sites only, an extra optical fiber was glued at the back of the shanks and protruded 100 μm below the shank tip (Fig. 2C). To maintain minimal shank thickness (15 μm) and guide the placement of the optical fibers, long 12 μm deep grooves were etched at the back of the shanks using a solid-state YAG laser-based laser micro-machining system (LaserMill, New Wave Research, Inc., Freemont, CA). Following the laser cut, the silicon grooves were fine polished at the very end of the shanks by chemically assisted focused Gallium ion beam milling using a dual beam FIB/SEM workstation (FEI DB-820). Liquid metal ion source based Gallium beam (30kV acceleration) current of 150pA at the sample surface was assisted by the Xenon difluoride (XeF_2) gas for chemically enhanced silicon etching of the shank substrate. The extra optical fibers were embedded and glued into the grooves using the same micro-manipulation procedure as described above. In our experience this arrangement does not compromise the recording quality of the silicon probe.

Rat experiments

Virus preparation and infection—Experiments with the microbial light-sensitive protein *Clamydomonas reinhardtii* Channelrodopsin-2 (ChR2) (Boyden et al., 2005; Han and Boyden, 2007; Ishizuka et al., 2006; Li et al., 2005; Nagel et al., 2003; Zhang et al., 2007) were carried out in rats. To obtain neuronal expression of ChR2 in the hippocampus, the CA1 region of 3-week old animals was injected with the adeno-associated virus (AAV) encoding ChR2-GFP fusion protein. Briefly, the fusion protein was cloned into an adeno-associated viral cassette containing the mouse synapsin promoter, a woodchuck post-transcriptional regulatory element (WPRE), SV40 poly-adenylation sequence, and two inverted terminal repeats. Viral particles were assembled using a modified helper-free system (Stratagene, La Jolla, CA) as a serotype 2/5 (*rep*/*cap* genes) AAV, and harvested and purified over sequential cesium chloride gradients as previously described (Grieger et al., 2006). The injections were performed stereotaxically under isofluorane anesthesia through a burr-hole above the dorsal hippocampus, using a glass pipette (10 μm tip size) connected to

a micro-injector (Nanoject II, Drummond Scientific Comp., Broomall, PA). 45 nl volumes (undiluted stock, minimum 10^{11} viral particles per ml) were injected every 300 μm between depths of 2.0 to 2.6 mm below dura, at 3 locations along CA1 septo-temporal axis (2.8-4.2 mm anterior, relative to bregma; 2.5-2.8 mm lateral).

Behavior training—Ten weeks after the virus injection, the rats were trained to run on an elevated figure 8 maze, built from the assembly of modular aluminum segments. Water rewards were delivered at 2 corners of the maze through water ports controlled by valves (Parker pneutronics #003-0130-900). Custom-made motorized doors forced the animals to take the right turns at the 2 intersections of the maze. Light beam sensing switches (McMaster #65845K7) detecting the animal's passages at some locations were used for the automatic triggers of valves, doors and laser for ChR2 activation.

Implantation surgery—Twelve weeks after the virus injection, the rats were prepared for chronic recordings. The general surgical procedures have been described (Fujisawa et al., 2007; Royer et al., 2010). Briefly, the prepared optrode assembly was attached to a micromanipulator. Two small watch-screws were driven into the bone above the cerebellum to serve as reference and ground electrodes. After enlarging the hole used for the virus injection, the dura mater was removed. The probe was positioned so that its shanks avoided puncturing large veins and inserted 1 mm into the brain. A warm mixture of wax and paraffin oil was applied in the hole around the shanks to protect the cortical surface and prevent cerebrospinal fluid from dehydrating and attaching to the shanks. The micromanipulator was cemented to the skull and a copper mesh cone was built around the entire assembly, to both protect and electrically shield the headgear.

Recording procedures—During a post-surgery recovery period of 1 week, the probe was lowered gradually until it reached the CA1 pyramidal layer. The animals were then recorded in the maze for ~30 min sessions, one or two sessions per day. During the recording sessions, a preamplifier (Plexon, Dallas, TX) was connected to the probe's output connector. For tracking the position of the animals, two small light-emitting diodes (5-cm separation) mounted above the headstage were recorded by a digital video camera.

Light modulation—A blue laser (473 nm; 60 mW; Aixiz) controlled by an analog input was used for ChR2 activation. The laser was collimated into a 6-meter long single mode optical fiber (Thorlabs custom patch cable) using a fiberport (Thorlabs #PAF-X-11-A). The other end of the optical fiber terminated into a LC connector, and connected to the optrode's LC connector via a LC-to-LC adapter (Thorlabs #ADALC1). Before implantation, the power of the laser at the tip of the optrode was measured with a power-meter (Melles Griot #13PEM001).

Mouse experiments

Virus preparation and injection—The NpHReGFP fusion protein was cloned into an adeno-associated viral cassette containing the mouse synapsin promoter, a woodchuck post-transcriptional regulatory element (WPRE), SV40 poly-adenylation sequence, and two inverted terminal repeats. rAAV-FLEX-*rev*-NpHReGFP (Atasoy et al., 2008) was assembled using a modified helper-free system (Stratagene, La Jolla, CA) as a serotype 2/7 (*rep*/*cap* genes) AAV, and harvested and purified over sequential cesium chloride gradients as previously described (Grieger et al., 2006). Using the same procedure as described for rats, the dorsal hippocampus of Parvalbumin-cre (PV-cre; Hippenmeyer et al., 2005) transgenic mice (3-5 weeks old) were injected at three sets of coordinates: 2.2, 2.4 and 2.7 mm posterior from bregma, and 2.1 mm from midline. 10-20 nl of virus was injected every

150 μm from 1.55 mm to 0.95 mm below pia. The pipette was held at 0.95 mm for 3 min before being completely retracted from the brain.

Preparation for head-fixed recordings—Mice were prepared for chronic recordings and trained to run for water reward with their heads fixed via a mounted head-plate into a stereotaxic device. Two small watch-screws were driven into the bone above the cerebellum to serve as reference and ground electrodes. A custom-fabricated platinum head-plate with a window opening above the left hippocampus was cemented to the skull with dental acrylic. After this surgery, the mice were trained for 2 weeks to run on a custom-built treadmill with their head fixed (40-min sessions per day). A water reward was delivered after every completed belt rotation through a licking port.

Recording procedures—The recordings were performed 3 to 6 weeks after the virus injection. On recording days, the mice were initially anesthetized with isofluorane and their head fixed. On the first day, the hole used for the virus injection was enlarged and the dura removed (on subsequent days the hole was simply cleaned with saline). The optrode assembly was fixed to a manipulator and lowered into the CA1 pyramidal layer. The hole was then sealed with liquid agar (1.5 %) applied at near body temperature. Aluminum foil was folded around the entire optrode assembly, which both served as a Faraday cage and prevented the mice from seeing the light emitted by the optical fibers. After reaching the CA1 pyramidal layer with the probe, mice were allowed to recover completely from the anesthesia. Recording sessions typically lasted for 1 hour, during which the animal's behavior alternated between periods of running and immobility. After each recording session, the probe was removed and the hole was filled with a mixture of bone wax and paraffin oil, and covered with silicon sealant (WPI, Kwik-sil). Each mouse was recorded for a maximum of 4 sessions (1 session per day).

Light modulation—A DPSS laser (561 nm; 100 mW; Crystalaser) controlled by TTL pulses was used for halorhodopsin activation. To adjust the intensity of the laser, a neutral density filter wheel was placed in front of the beam. An optrode with 4 optical fibers was used (Fig. 2B), therefore the laser beam was first split with beam splitters (ThorLabs #CM1-BS1) and diverted by reflecting mirrors (Thorlabs #CM1-P01) into 4 separate fiber ports (ThorLabs #PAF-X-7-A). Long single-mode optical fibers connected the fiber ports to the OPTRODE fibers as described for the rat experiments.

Behavior control, data acquisition and analysis

The behavior hardware (valves, motorized doors and light beam sensing switches) and the laser power supply were connected to a computer board (National Instruments #NI PCI-6221) and controlled by custom-made LabView (National Instruments) and Python programs. Neurophysiological signals were acquired continuously at 32.552 kHz on a 128-channel DigiLynx system (Neuralynx, Inc). The wideband signals were digitally high-pass filtered (0.8-5kHz) offline for spike detection or low-pass filtered (0-500 Hz) and down sampled to 1.252 kHz for local field potentials. Spike sorting was performed semi-automatically, using KlustaKwik (available at: http://osiris.rutgers.edu/buzsaki/software), followed by manual adjustment of the clusters (Harris et al., 2000). Additional data analysis was done using custom Matlab routines.

Light stimulation of neurons

Spike detection during ChR2 activation—A well-known problem with short electric pulses, typically used for stimulation, is that they activate the neurons in a highly synchronous manner. As a result, spike waveforms of nearby neurons get superimposed and blended into population spikes (complex waveforms), and isolation of single neurons by

clustering methods using spike waveform features becomes compromised. The same problem is expected when using short light pulses to activate ChR2-expressing neurons. However, in contrast to electrical stimulation, longer stimulus waveforms can be used for light excitation of ChR2. In particular, slowly rising waveforms of light might activate the cells at different times because of differences in activation thresholds, making spike separation possible. To test this hypothesis, we compared the effects of sine wave patterns (5Hz) versus short pulses of light (5 ms duration, every 1 s). The experiments were performed in the CA1 hippocampal region of rats using the optrode device shown in Figure 2A. The effect of both stimulation regimes could be seen on the wideband signal (Fig. 4A and Fig. 5A). High intensity light stimulation occasionally caused an artifactual potential via the photoelectric effect of the light on the conducting wires of the probe (Han et al., 2009). This artifact could also be detected in brain tissue without ChR2 expression, such as the neocortex overlying the hippocampus, and could therefore be subtracted from the recorded signal. Following the implementation of spike detection and separation (Fig. 4C), the activation of several cells by the sine wave stimulus was readily detectable in the neurons' spike raster plot (Fig. 4A), spike autocorrelograms (Fig. 4C; note the rhythmic oscillation at the 5 Hz stimulus frequency), and peri-stimulus spike time histograms (Fig. 5C). Both the number of excited neurons and the magnitude of the responses increased with the intensity of the stimulus (Fig. 5C and D). In contrast, activation of clustered neurons by light pulses was often not detectable, even in neurons, which showed a reliable response to the sine wave stimuli (Fig. 5C and D). This did not result from a failure of the light pulse to excite the neurons, since waveforms of superimposed spikes were visible on the wideband signal during the pulses (Fig. 5B), and activation of the network was obvious from the strong inhibitory responses of putative interneurons (Fig. 5C, 5th row). Instead, a failure to isolate the spikes triggered by the light pulses, due to superimposition of spike waveforms, is most likely the cause.

Spatial extent of light stimulation—Because the optical fiber terminated ~100 μm above the recording sites (Fig. 2A), the stimulation was restricted to a small portion of the monitored tissue. As anticipated, the effect of the stimulation was typically observed on the shank carrying the optical fiber. This specificity was visible on both the wideband signals (Fig. 6A) and the responses of single neurons (Fig. 6B and D). At low stimulus intensity of 50 μW, neuronal spikes were elicited only in neurons recorded by the shank with the optical fiber (Fig. 6B, left panel). After the intensity was raised to 100 μW, neurons recorded by the adjacent shank (250 μm away) could also be activated occasionally (Fig. 6B, right panel, and D). Both direct light activation or indirect synaptic activation could be the origin of these distant neurons responses, although occurrence of the latter should be rare given the sparsity of excitatory connections between CA1 pyramidal cells (Amaral and Witter, 1989).

Figure 7 shows an example of transient stimulation of a selected set of the monitored neurons during maze behavior. In this experiment, the laser was turned on (5 Hz sinus pattern) when the animal was in a selected part of the maze (Fig. 7B) on every other trial. In addition to the neurons' place fields, light induced firing could be observed in 3 of the place cells recorded by the shank with an optical fiber (Fig. 7C, red arrows).

Cell type specific light stimulation—Because ChR2 or halorhodopsin expression can be restricted to genetically specific cell types (Moore et al., 2009; Sohal et al., 2009), a main advantage of optical stimulation is the possibility to affect only neurons of a selective type. In this respect, the optrode can be a powerful tool to study the contribution of specific cell types to the local network dynamic. For example, neurons of a specific type can be identified among the numerous recorded neurons from their response to light, and subsequently, their firing pattern can be analyzed in relation to the firing of other neurons,

LFP patterns and the animal's behavior. In addition, the impact of their stimulation/inhibition on the rest of the network can be monitored.

Figure 8 shows the light responses of cells recorded simultaneously in the CA1 hippocampal area of a halo/PV-CRE mouse. Parvalbumin expressing cells can be readily identified by their fast square-shape inhibition caused by the light pulses. Their firing rate is relatively high, as expected, since most parvalbumin expressing neurons are known to be fast-spiking GABAergic interneurons (Freund and Buzsaki, 1996). In contrast, many cells showed an increased firing rate, presumably as a result of their disinhibition following the suppression of PV neuron firing.

Discussion

We described a procedure for the fabrication of optoelectronic probes (optrodes), tools that combine the advantages of optogenetics and silicon probes, enabling both fine scale stimulation and large-scale recording of neurons in behaving animals. A key advantage of these devices is the enhanced spatial precision of stimulation that is achieved by delivering light close to the recording sites of the probe. Additional cell-type specificity is achieved through genetic targeting of the light-activated current sources. Our experimental findings illustrate these capabilities.

Microstimulation is an important tool for investigating the contribution of small groups of neurons to the network patterns (Salzman et al., 1990; Cohen and Newsome, 2004; Butovas et al., 2006; Butovas and Schwarz, 2003; Seidemann et al., 2002). For this purpose, electrical stimulation has some limitations. First, it generates local electrical artifacts that are typically larger than the extracellular spike signals, requiring complex methods to extract the neuronal waveforms (Olsson et al., 2005). Second, it activates neurons in a highly synchronous manner, preventing the reliable isolation of individual neuron by clustering methods for large-scale recordings. The induced synchronous discharge is also more effective at synaptically activating other neurons (Csicsvari et al., 1998; Fujisawa et al., 2007), making the separation of direct and synaptically mediated effects difficult in recurrent networks. Third, even very low stimulus intensities can recruit distant neurons through direct axonal stimulation (Histed et al., 2009), preventing the ability to perform stimulations of high spatial resolution. Although the use of the optogenetic tools discussed here can largely eliminate most of these shortcomings, a number of precautions should be taken. First, although the passive structure of axons makes them relatively harder to activate with ChR2 than soma-dendrite regions (Johnston and Wu, 1995), ChR2 expression can potentially be high enough in axons for them to be directly excited by light stimuli (Petreanu et al., 2007 and 2009). Therefore neurons can still be recruited via antidromic axon stimulation by brief large amplitude light pulses. Second, brief light pulses also tend to synchronously activate ChR2-expressing neurons, with the associated issues mentioned above.

The problem of synchrony-induced spike superimposition can be avoided through the use of low frequency sine wave stimuli. The 5 Hz sinusoid stimulation used here, close to the natural theta oscillation frequency of the hippocampal networks, eliminated the induction of population spikes and did not alter the spike waveforms. As a result, light-activated pyramidal neurons could be readily identified following spike sorting by routine clustering methods. In addition, the use of sine wave stimuli should lower the chance of indirect synaptic activation of pyramidal cells because of the non-synchronized discharges they generate compared to short pulses. In our experiments, the chance of indirect synaptic activation was low because of the sparse recurrent collateral between CA1 principal neurons (Amaral and Witter, 1989). Finally, we speculate that slow stimulus waveforms should

further reduce the chances of axonal stimulation at light levels sufficient to activate somata. Indeed, since the somata have higher low-pass filtering properties than axons, the impact of light-induced potentials should be relatively decreased in somata when using fast frequency stimuli, but not for slow frequency stimuli.

Silencing of neuronal populations is particularly advantageous for the dissection of network components. For the identification of neuron types, light suppression of halorhodopsin-expressing neurons (Han and Boyden, 2007; Zhang et al., 2007) should be the preferred method since it avoids the synchrony-induced spike superimposition problem and makes the separation of direct and synaptically mediated effects straightforward. Yellow light pulses robustly silenced PV-containing interneurons in our experiments. Although synaptically-mediated disinhibitory effects of pyramidal cells and other putative interneurons were evident in several experiments, suppression of activity for the entire duration of stimulation is expected to occur only in halorhodopsin-expressing neurons.

Conclusions

We have described the fabrication of highly versatile devices that allow for the simultaneous recording of large numbers of neurons and the optical activation/silencing of select sub-populations of neurons within the recorded area. These devices can be used in any brain area that is accessible to thin silicon probes and are suitable for both anesthetized and awake recording conditions in behaving animals. When paired with the expression of light sensitive actuators within genetically specified neuronal populations, these devices allow the relatively straightforward and interpretable manipulation of network activity. Future development of optoelectronic probes may include the use of light emitting diode (LED)-coupled fibers, waveguides for light in the silicon probe substrate and on-site organic-LEDs, combined to further decrease probe volume.

References

Amaral DG, Witter MP. The three-dimensional organization of the hippocampal formation: a review of anatomical data. Neuroscience. 1989; 31:571–591. [PubMed: 2687721]

Atasoy D, Aponte Y, Su HH, Sternson SM. A FLEX switch targets Channelrhodopsin-2 to multiple cell types for imaging and long-range circuit mapping. J Neurosci. 2008; 28:7025–7030. [PubMed: 18614669]

Bartho P, Hirase H, Monconduit L, Zugaro M, Harris KD, Buzsaki G. Characterization of neocortical principal cells and interneurons by network interactions and extracellular features. J Neurophysiol. 2004; 92:600–608. [PubMed: 15056678]

Battaglia FP, Kalenscher T, Cabral H, Winkel J, Bos J, Manuputy R, van Lieshout T, Pinkse F, Beukers H, Pennartz C. The Lantern: an ultra-light micro-drive for multi-tetrode recordings in mice and other small animals. J Neurosci Methods. 2009; 178:291–300. [PubMed: 19152807]

Boyden ES, Zhang F, Bamberg E, Nagel G, Deisseroth K. Millisecond-timescale, genetically targeted optical control of neural activity. Nat Neurosci. 2005; 8:1263–1268. [PubMed: 16116447]

Butovas S, Hormuzdi SG, Monyer H, Schwarz C. Effects of electrically coupled inhibitory networks on local neuronal responses to intracortical microstimulation. J Neurophysiol. 2006; 96:1227–1236. [PubMed: 16837655]

Butovas S, Schwarz C. Spatiotemporal effects of microstimulation in rat neocortex: a parametric study using multielectrode recordings. J Neurophysiol. 2003; 90:3024–3039. [PubMed: 12878710]

Buzsaki G. Large-scale recording of neuronal ensembles. Nat Neurosci. 2004; 7:446–451. [PubMed: 15114356]

Buzsaki G, Horvath Z, Urioste R, Hetke J, Wise K. High-frequency network oscillation in the hippocampus. Science. 1992; 256:1025–1027. [PubMed: 1589772]

Cardin JA, Carlén M, Meletis K, Knoblich U, Zhang F, Deisseroth K, Tsai LH, Moore CI. Driving fast-spiking cells induces gamma rhythm and controls sensory responses. Nature. 2009; 459:663–667. [PubMed: 19396156]

Cohen MR, Newsome WT. What electrical microstimulation has revealed about the neural basis of cognition. Curr Opin Neurobiol. 2004; 14:169–177. [PubMed: 15082321]

Csicsvari J, Henze DA, Jamieson B, Harris KD, Sirota A, Bartho P, Wise KD, Buzsaki G. Massively parallel recording of unit and local field potentials with silicon-based electrodes. J Neurophysiol. 2003; 90:1314–1323. [PubMed: 12904510]

Csicsvari J, Hirase H, Czurko A, Buzsaki G. Reliability and state dependence of pyramidal cell-interneuron synapses in the hippocampus: an ensemble approach in the behaving rat. Neuron. 1998; 21:179–189. [PubMed: 9697862]

Deisseroth K, Feng G, Majewska AK, Miesenbock G, Ting A, Schnitzer MJ. Next-generation optical technologies for illuminating genetically targeted brain circuits. J Neurosci. 2006; 26:10380–10386. [PubMed: 17035522]

Freund TF, Buzsaki G. Interneurons of the hippocampus. Hippocampus. 1996; 6:347–470. [PubMed: 8915675]

Fujisawa S, Amarasingham A, Harrison MT, Buzsaki G. Behavior-dependent short-term assembly dynamics in the medial prefrontal cortex. Nat Neurosci. 2008; 11:823–833. [PubMed: 18516033]

Gelbard-Sagiv H, Mukamel R, Harel M, Malach R, Fried I. Internally generated reactivation of single neurons in human hippocampus during free recall. Science. 2008; 322:96–101. [PubMed: 18772395]

Grieger JC, Choi VW, Samulski RJ. Production and characterization of adeno-associated viral vectors. Nat Protoc. 2006; 1:1412–1428. [PubMed: 17406430]

Han X, Boyden ES. Multiple-color optical activation, silencing, and desynchronization of neural activity, with single-spike temporal resolution. PLoS One. 2007; 2:e299. [PubMed: 17375185]

Han X, Qian X, Bernstein JG, Zhou HH, Franzesi GT, Stern P, Bronson RT, Graybiel AM, Desimone R, Boyden ES. Millisecond-timescale optical control of neural dynamics in the nonhuman primate brain. Neuron. 2009; 62:191–198. [PubMed: 19409264]

Harris KD, Csicsvari J, Hirase H, Dragoi G, Buzsaki G. Organization of cell assemblies in the hippocampus. Nature. 2003; 424:552–556. [PubMed: 12891358]

Harris KD, Henze DA, Csicsvari J, Hirase H, Buzsaki G. Accuracy of tetrode spike separation as determined by simultaneous intracellular and extracellular measurements. J Neurophysiol. 2000; 84:401–414. [PubMed: 10899214]

Hippenmeyer S, Vrieseling E, Sigrist M, Portmann T, Laengle C, Ladle DR, Arber S. A developmental switch in the response of DRG neurons to ETS transcription factor signaling. PLoS Biol. 2005; 3:e159. [PubMed: 15836427]

Histed MH, Bonin V, Reid RC. Direct activation of sparse, distributed populations of cortical neurons by electrical microstimulation. Neuron. 2009; 63:508–522. [PubMed: 19709632]

Ishizuka T, Kakuda M, Araki R, Yawo H. Kinetic evaluation of photosensitivity in genetically engineered neurons expressing green algae light-gated channels. Neurosci Res. 2006; 54:85–94. [PubMed: 16298005]

Johnston, D.; Wu, S. Foundations of cellular neurophysiology. MIT Press; Cambridge, MA: 1995. p. 60-84.

Kipke DR, Shain W, Buzsaki G, Fetz E, Henderson JM, Hetke JF, Schalk G. Advanced neurotechnologies for chronic neural interfaces: new horizons and clinical opportunities. J Neurosci. 2008; 28:11830–11838. [PubMed: 19005048]

Klausberger T, Magill PJ, Marton LF, Roberts JD, Cobden PM, Buzsaki G, Somogyi P. Brain-state- and cell-type-specific firing of hippocampal interneurons in vivo. Nature. 2003; 421:844–848. [PubMed: 12594513]

Klausberger T, Somogyi P. Neuronal diversity and temporal dynamics: the unity of hippocampal circuit operations. Science. 2008; 321:53–57. [PubMed: 18599766]

Li X, Gutierrez DV, Hanson MG, Han J, Mark MD, Chiel H, Hegemann P, Landmesser LT, Herlitze S. Fast noninvasive activation and inhibition of neural and network activity by vertebrate

rhodopsin and green algae channelrhodopsin. Proc Natl Acad Sci USA. 2005; 102:17816–17821. [PubMed: 16306259]

Markram H, Toledo-Rodriguez M, Wang Y, Gupta A, Silberberg G, Wu C. Interneurons of the neocortical inhibitory system. Nat Rev Neurosci. 2004; 5:793–807. [PubMed: 15378039]

Nagel G, Szellas T, Huhn W, Kateriya S, Adeishvili N, Berthold P, Ollig D, Hegemann P, Bamberg E. Channelrhodopsin-2, a directly light-gated cation-selective membrane channel. Proc Natl Acad Sci USA. 2003; 100:13940–13945. [PubMed: 14615590]

O'Connor DH, Huber D, Svoboda K. Reverse engineering the mouse brain. Nature. 2009; 461:923–929. [PubMed: 19829372]

Olsson RH 3rd, Buhl DL, Sirota AM, Buzsaki G, Wise KD. Band-tunable and multiplexed integrated circuits for simultaneous recording and stimulation with microelectrode arrays. IEEE Trans Biomed Eng. 2005; 52:1303–1311. [PubMed: 16041994]

Pastalkova E, Itskov V, Amarasingham A, Buzsaki G. Internally generated cell assembly sequences in the rat hippocampus. Science. 2008; 321:1322–1327. [PubMed: 18772431]

Petreanu L, Huber D, Sobczyk A, Svoboda K. Channelrhodopsin-2-assisted circuit mapping of long-range callosal projections. Nat Neurosci. 2007; 10:663–668. [PubMed: 17435752]

Petreanu L, Mao T, Sternson SM, Svoboda K. The subcellular organization of neocortical excitatory connections. Nature. 2009; 457:1142–1145. [PubMed: 19151697]

Rizk M, Bossetti CA, Jochum TA, Callender SH, Nicolelis MA, Turner DA, Wolf PD. A fully implantable 96-channel neural data acquisition system. J Neural Eng. 2009; 6:026002. [PubMed: 19255459]

Royer, S.; Andrasfalvy, BK.; Magee, J.; Buzsaki, G. Light activation and detection of hippocampal neurons in the behaving rat. Society for Neuroscience; 2008. Abstract #435.10/I3

Royer S, Sirota A, Patel J, Buzsaki G. Distinct representations and theta dynamics in dorsal and ventral hippocampus. J Neurosci. 2010

Salzman CD, Britten KH, Newsome WT. Cortical microstimulation influences perceptual judgements of motion direction. Nature. 1990; 346:174–177. [PubMed: 2366872]

Seidemann E, Arieli A, Grinvald A, Slovin H. Dynamics of depolarization and hyperpolarization in the frontal cortex and saccade goal. Science. 2002; 295:862–865. [PubMed: 11823644]

Sohal VS, Zhang F, Yizhar O, Deisseroth K. Parvalbumin neurons and gamma rhythms enhance cortical circuit performance. Nature. 2009; 459:698–702. [PubMed: 19396159]

Wilson MA, McNaughton BL. Dynamics of the hippocampal ensemble code for space. Science. 1993; 261:1055–1058. [PubMed: 8351520]

Wise KD, Najafi K. Microfabrication techniques for integrated sensors and microsystems. Science. 1991; 254:1335–1342. [PubMed: 1962192]

Yamamoto J, Wilson MA. Large-scale chronically implantable precision motorized microdrive array for freely behaving animals. J Neurophysiol. 2008; 100:2430–2440. [PubMed: 18667539]

Zhang F, Aravanis AM, Adamantidis A, de Lecea L, Deisseroth K. Circuit-breakers: optical technologies for probing neural signals and systems. Nat Rev Neurosci. 2007a; 8:577–581. [PubMed: 17643087]

Zhang F, Wang LP, Brauner M, Liewald JF, Kay K, Watzke N, Wood PG, Bamberg E, Nagel G, Gottschalk A, Deisseroth K. Multimodal fast optical interrogation of neural circuitry. Nature. 2007b; 446:633–639. [PubMed: 17410168]

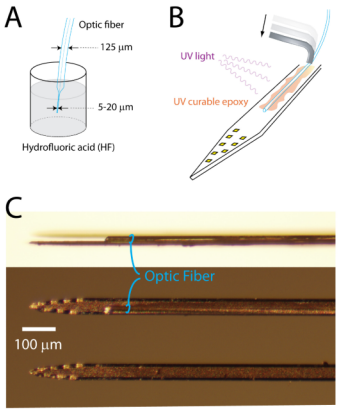

Figure 1.

Procedure for integrating optical fibers on silicon probe shanks. A. Etching of the optical fiber. B. Fixing the fiber on the shank. The fiber is flattened on the shank by pushing it (arrow) with a bent piece of metal micro-tube. Epoxy glue is applied and then cured with UV light. C. Image of shanks with (upper 2) and without (bottom) a glued optical fiber. The picture on top is a side view of the shank while the 2 others are front views.

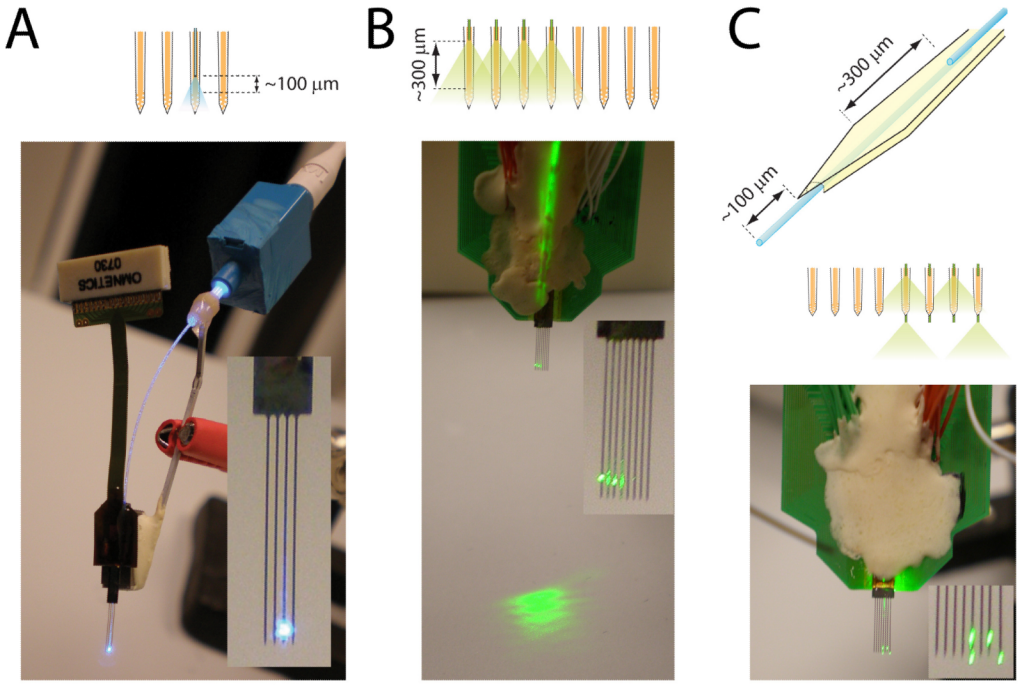

Figure 2.

Examples of fiber-based optoelectronic probe designs. A. Four-shank silicon probe with one of its shank equipped with an optical fiber. The scheme above the picture shows the configuration of the optical fiber and shanks. The back end of the fiber is glued in the ferrule of a LC connector, and is plugged into a LC to LC adaptor cut in half (blue plastic cubic piece). Inset: Zoom on the shanks. B. Same as A for an 8-shank silicon probe equipped with 4 optical fibers. C. Same as A for a silicon probe equipped with 2 optical fibers per shank. Only 4 of the optical fibers were lighted on for better clarity of the picture.

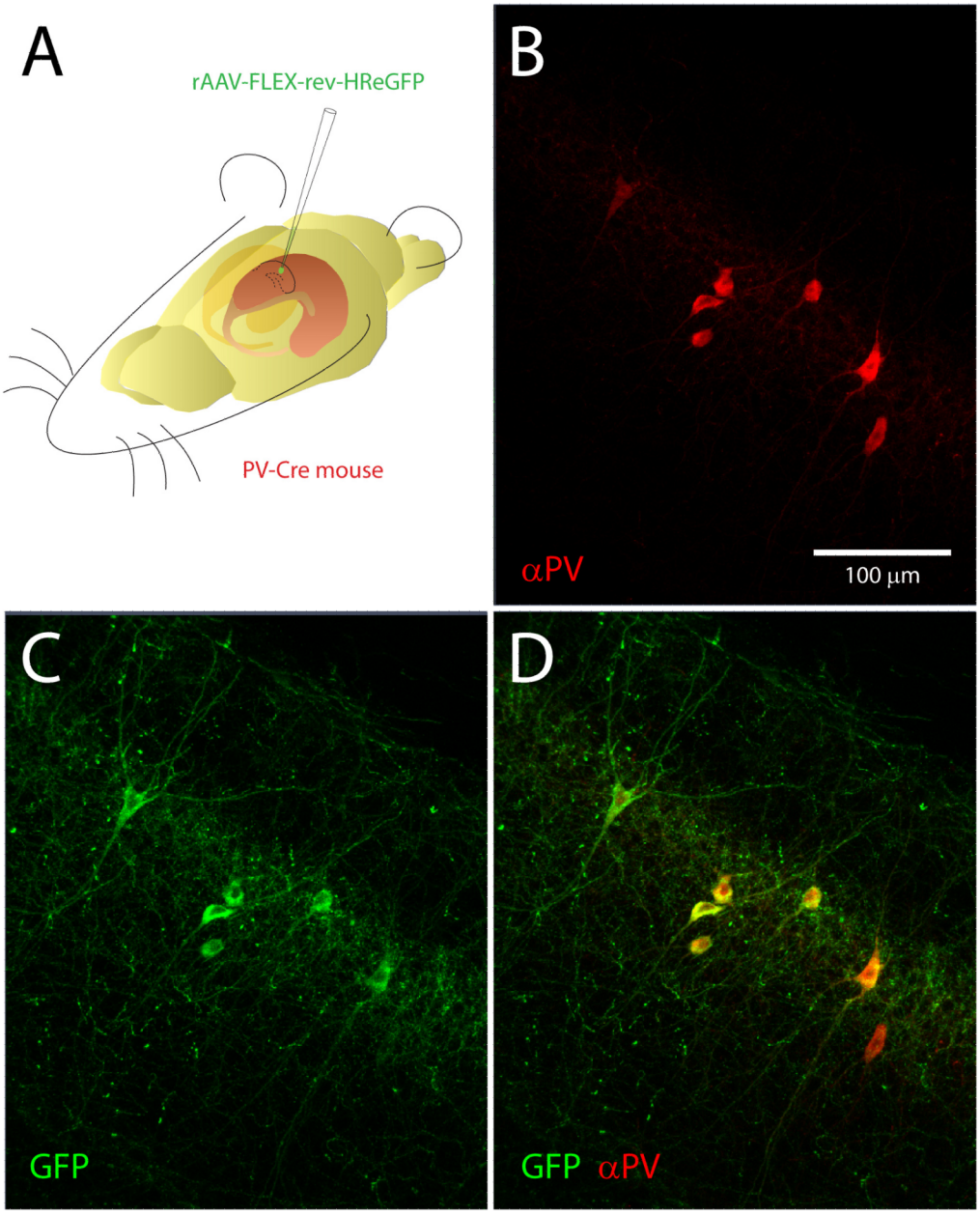

Figure 3.

Halorhodopsin expression in parvalbumin-positive hippocampal neurons. A. rAAV SYN-rev-NpHRe-GFP virus was injected into the CA1 region of PV-Cre mouse hippocampus. B. Immunolabeling of parvalbumin-positive neurons. C. Cre-dependent expression of Halorhodopsin-GFP in interneurons following viral injection. D. Merged images demonstrate that halorhodopsin is expressed exclusively in parvalbumin-positive neurons.

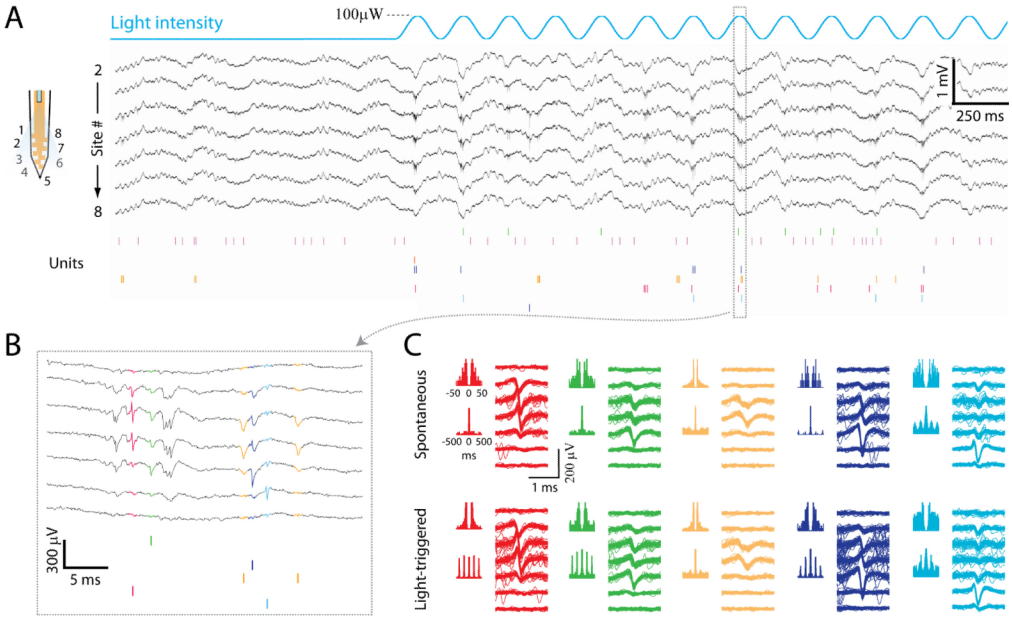

Figure 4.

Excitation of ChR2 infected neurons by sine wave pattern of light stimulus. A. Wideband signals (black traces) and raster plot of unit activity (colored bars) recorded from the shank equipped with optical fiber, before and during a 5 Hz sine wave stimulus pattern (top blue line). Only wideband signals of functional channels are displayed. The scheme on the left shows the positions of the recording sites for the corresponding traces numbers. B. Expansion of the excitation cycle indicated in A. The waveforms of the spikes are the same colors as in the raster plots. C. Spike autocorrelograms at two time scales and spike waveforms on each recording channel for 5 isolated neurons, during spontaneous activity (upper) and light stimulation (lower). Same neurons and colors as in A and B. Note the highly rhythmic autocorrelograms of the red, green and dark blue neurons (lower panel), reflecting their entrainment by the light stimuli.

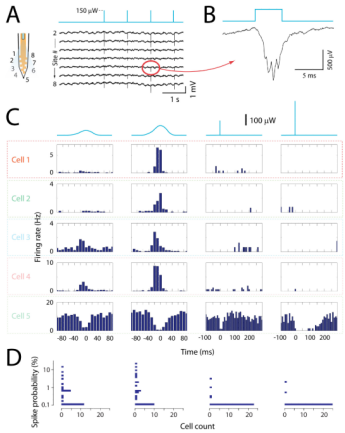

Figure 5.

Comparison of sine wave and short pulse stimuli. A. Wideband signals recorded from the shank equipped with optical fiber, before and during a 1 Hz stimulus pattern of 5 ms duration pulses (top blue line). The scheme on the left shows the positions of the recording sites for the corresponding traces numbers. B. Expanded view of one channel's response to the light pulse. C. Each row shows the peri-stimulus histograms of one neuron's firing during sine wave or pulse stimuli. The blue traces on top represent the stimulus waveform. Note that the sine wave stimulus has not exactly a sinus shape because of the non-linear relationship between the laser's voltage command and intensity output. The time zero corresponds to the peak of the sine waves or to the onset of the pulses. The 5th neuron is a putative interneuron based on its high firing rate. D. Horizontal histograms of response amplitudes for all neurons. Each histogram is aligned to the corresponding stimulus in C. The y axis is the probability that a stimulus evokes a spike.

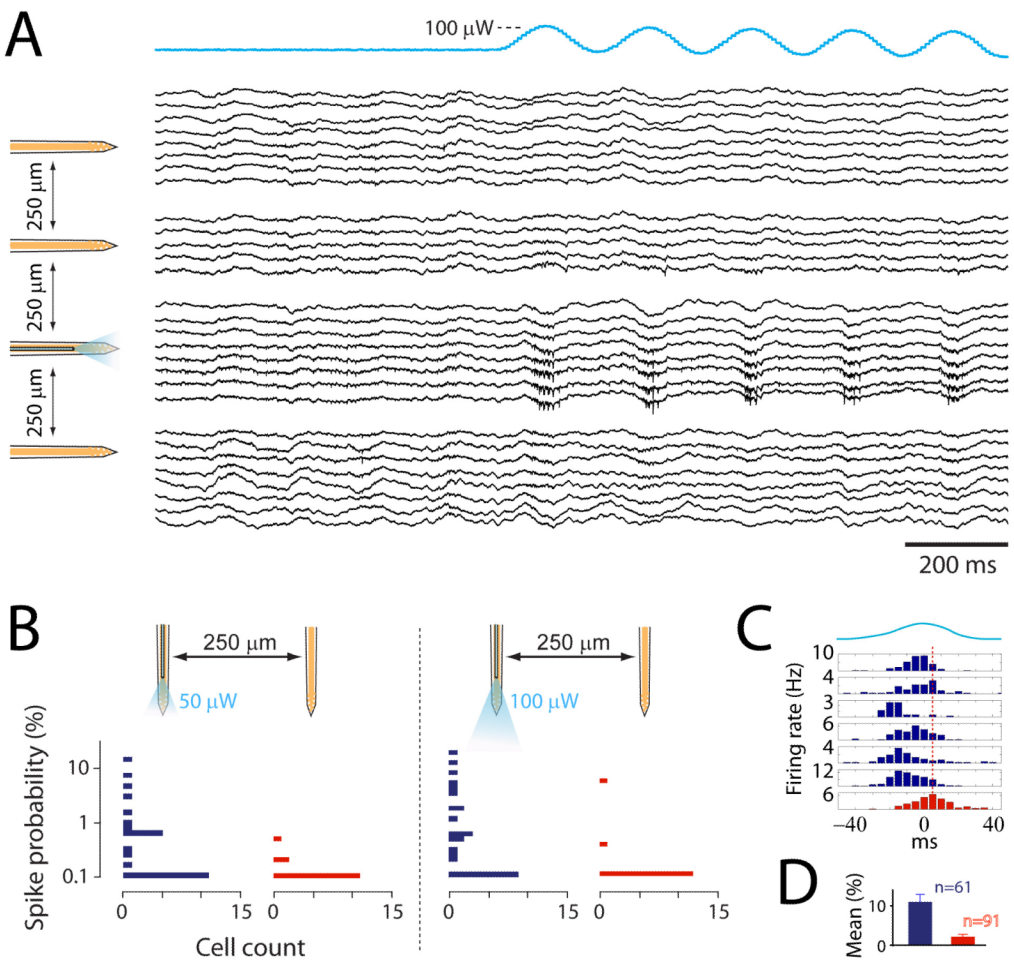

Figure 6.

Spatial resolution of the stimulation. A. Wideband signals recorded from all shanks of the optoelectronic probe. The traces are grouped and aligned to their corresponding shank (schemed on the left). Only functional channels are displayed. Note the apparition of unit activity selectively on the shank with optical fiber as the light stimulation (blue trace on top) is turned on. B. Horizontal histograms of responses amplitudes of neurons recorded on the shank with optical fiber (blue bars) and on the neighboring shank (red bars), for two levels of light intensity. The y axis is the probability that a stimulus evokes a spike. C. Peri-stimulus histograms of activated neurons on the shank with optical fiber (blue) and of one activated neuron on the neighboring shank (red). The blue trace on top represents the stimulus waveform. The red dashed line indicates the peak time of the red histogram. D. Mean increase of spikes neurons recorded on the shank with optical fiber (blue bar, n=61; mean+SE) and on the neighboring shank (red bar, n=91; mean+SE; statistical difference to blue bar: $P<0.001$; unpaired t-test). Neurons from 2 rats and 8 recording sessions are included.

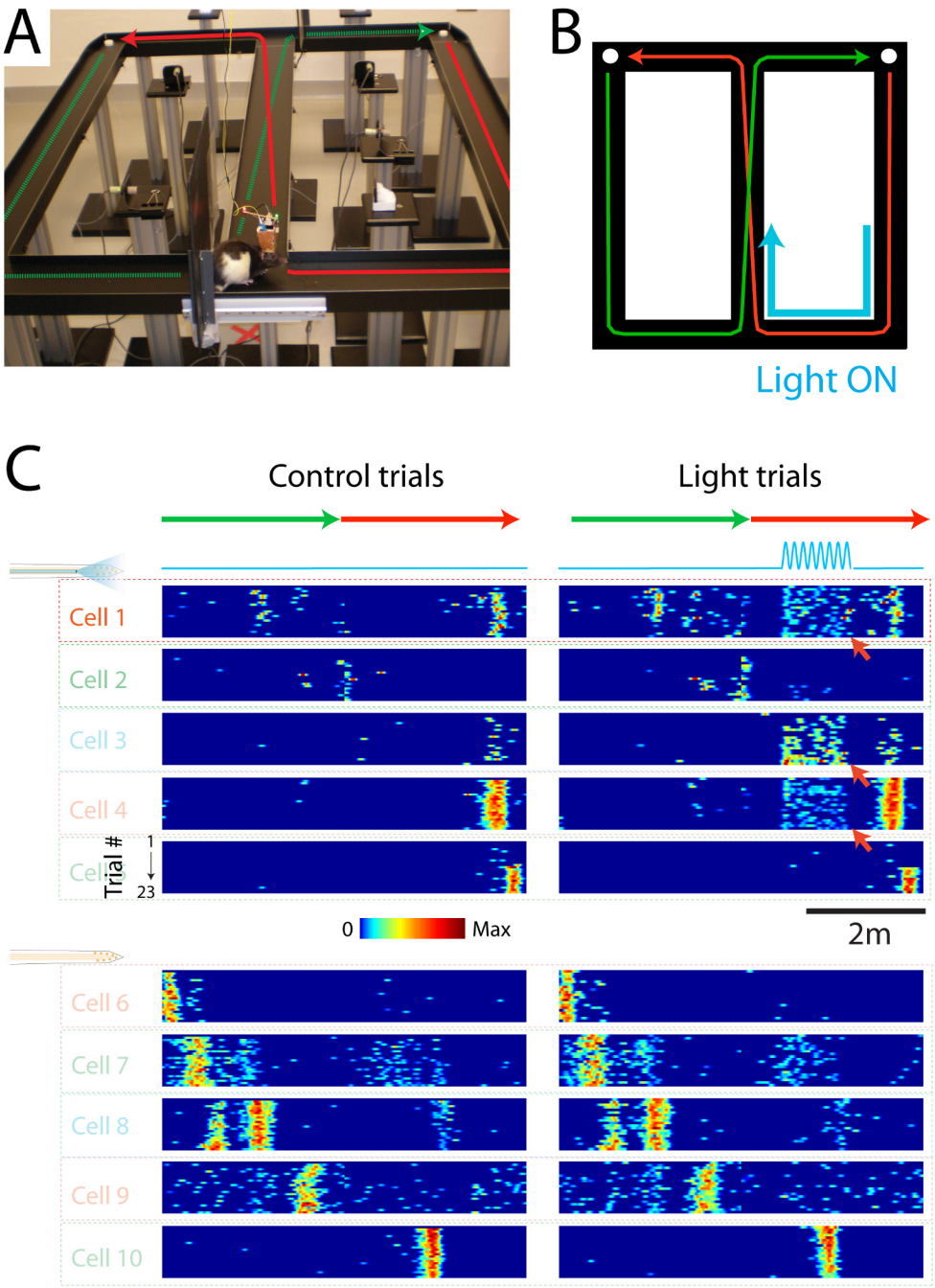

Figure 7.

Position dependent stimulation of a subgroup of neurons. A. Picture of the maze and implanted rat. The green and red arrows depict the trajectory of the animal from one water port to the other. B. Scheme of the maze and animal trajectory (green and red arrows). The blue arrow indicates the part of trajectory during which the laser was turned on. C. Color-coded plots of the neurons firing fields. Each plot shows one neuron's color-coded firing rate as a function of the animal linear position (green and red arrows on top). Different trials are represented in the rows of each plot. The left and right plots are the same neurons, for control trials (left) and trials with light stimulation (right, blue line). Red arrows point at neurons, which responded to light stimulation. The 5 upper neurons were recorded on the

shank with the optical fiber while the 5 lower neurons were recorded on the neighboring shank.

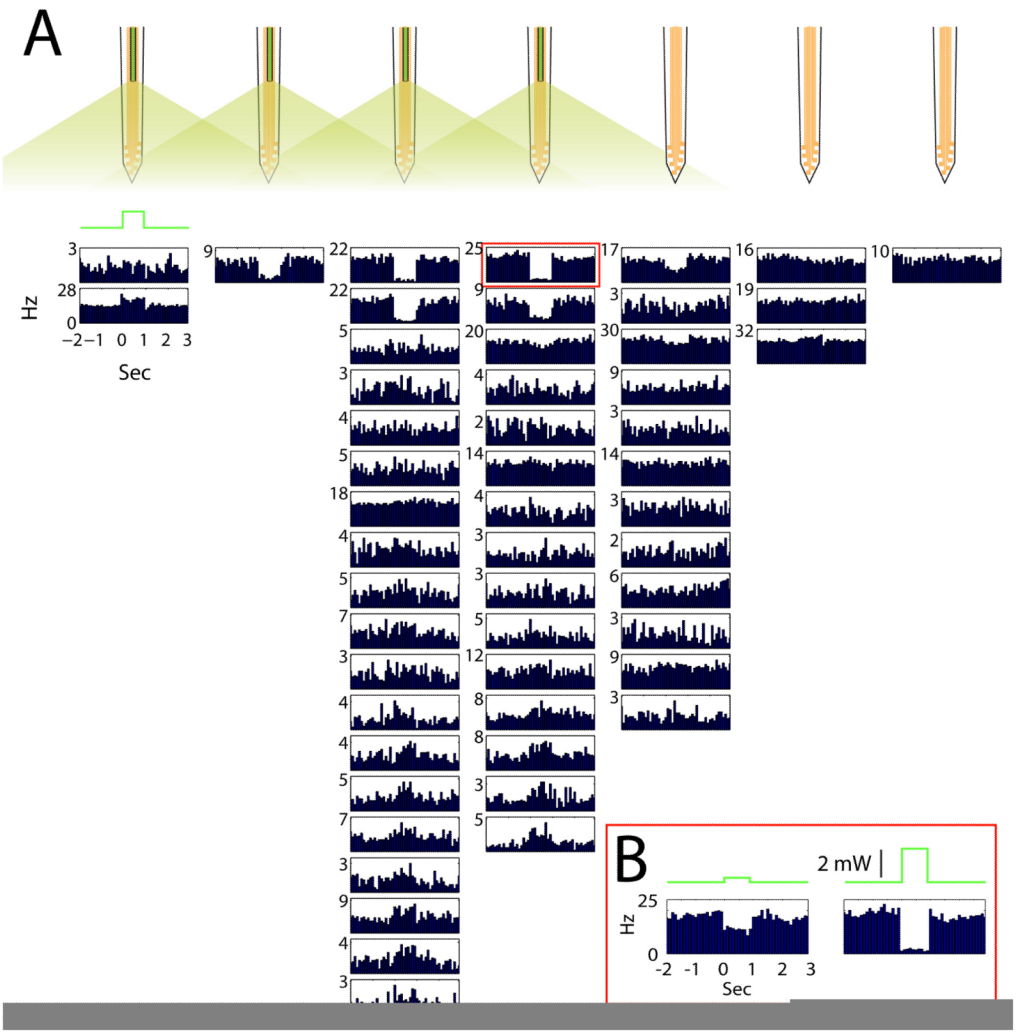

Figure 8.
Halorhodopsin-mediated inhibition of parvalbumin neurons. A. Peri-stimulus histograms of neuronal responses to 1-second long light pulses (green trace). All neurons were recorded simultaneously by an 8-shank optoelectronic probe (Fig. 2B). Each histogram is aligned to the shank the neuron was recorded from (scheme on top). B. Light intensity dependence of spike suppression.